

Magnetically tunable visible reflectivity utilizing the electron accumulation in indium-tin-oxide waveguide layer with subwavelength grating

Y. Okano^a, Y. Takashima^{*b}, M. Haraguchi^{b,c}, Y. Naoi^{b,c}

^aGraduate School of Advanced Technology and Science, Tokushima University; ^bGraduate School of Technology and Science, Tokushima University; ^cInstitute of Post-LED Photonics, Tokushima University, 2-1 Minami-josanjima, Tokushima, Japan

ABSTRACT

Magnetic field detection was experimentally demonstrated utilizing the optical spectral change of Al-subwavelength grating (SWG) on indium-tin-oxide (ITO) layer. The Al-SWG was fabricated on the ITO layer by electron-beam lithography technique. The fabricated sample shows the peak in the reflection spectrum resulting from the excitation of guided-mode in ITO layer. Electron accumulation layer in ITO was induced by applying magnetic field and flowing current, and the accumulation layer decreased the reflection peak intensity. As the magnetic field of 172 mT was applied, the intensity decreasing reached to 3 % of that without magnetic field. The intensity returned to the original value before measurement when the magnetic field and the current disappeared. These results indicate that our structure can detect tens of mT magnetic field without degaussing.

Keywords: Subwavelength grating, waveguide, ITO, magnetic field sensor

1. INTRODUCTION

Sensing techniques play very important role in internet of things (IoT) society. In particular, the magnetic field sensing is one of the most widely used technique for huge application fields, such as position sensing, current sensing, bio-sensing, nuclear fusion monitor. For realizing these IoT applications, the magnetic field sensor with high sensitivity, compact size, real-time detection, and stability of electromagnetic noises is suitable.

To achieve high sensitivity, the several electrical magnetic field sensors using Hall and giant-magnetic-resistive effects have been developed and widely used^{1, 2}. Several groups have reported extremely high sensitivity for magnetic field utilizing super-quantum-interference-devices³. However, the sensitivities of the electrical sensors are generally influenced by the electromagnetic noises because the sensors directly measure voltage or current for the detection of magnetic field. The influence of the electromagnetic noises on the sensitivity restricts the practical application fields of the sensors.

Recently, optical sensors for magnetic field attracted much interest because the optical sensors possess high stability for electromagnetic noises and quick response time. Many types of optical magnetic field sensors were developed using magnetic fluid photonic crystal fiber⁴, Bragg fiber⁵, structured fiber⁶, and interferometer⁷. The optical sensors require no electrical wiring and are very suitable for compact integrated applications. However, the sensors required the specialized optical setups and structural geometry with magnetic fluid.

In our previous reports, we realized the optical magnetic field sensor Ni subwavelength grating (SWG) without cumbersome optical system⁸⁻¹⁰. The Ni-SWG based sensor can detect tens of mT magnetic field with very simple normal incidence. However, the sensor required degaussing at each magnetic field measurements owing to hysteresis of the magnetization of Ni, and this is obstacle for ease of usage of the sensor. In this work, we demonstrated degaussing-free magnetic field sensor using an Al-SWG on an indium-tin-oxide (ITO) waveguide layer. We proposed the new magnetic field sensing concept utilizing combination of the guided-mode and electron accumulation in ITO waveguide layer. Our proposed sensor was fabricated by electron-beam (EB) lithography and evaporation techniques.

*takashima@tokushima-u.ac.jp; phone +81-88-656-7447; fax +81-88-656-7447

The peak originated from the guided-mode excitation was obtained in the normal reflection spectrum of the fabrication sample. The peak reflectivity decreased when the external magnetic field up to 172 mT was applied during the current flowing into ITO layer, and the relative decreasing of the reflectivity reached to 3% of that without the current and the magnetic field. When the current and magnetic field disappeared, the reflection peak intensity almost returned to the original value before current flowing and magnetic field applying. Moreover, we calculated the electromagnetic field distribution of our sample by finite-difference time-domain (FDTD) method and discussed the influence of the electron accumulation layer on the guided-mode in ITO layer.

2. DESIGN AND FABRICATION OF OUR STRUCTURE

In this section, we describe the design concept of our proposed sensor. Figure 1 shows the schematic of the proposed sensor. The Al-SWG with period Λ is arranged on the ITO layer deposited on glass substrate. The structural parameter symbols t_{ITO} , t_{SWG} , w , represent ITO layer thickness, SWG thickness, and SWG bar width, respectively. The incident plane wave enters normally into the sensor. The incident light is p-polarized (the electric field is perpendicular to the SWG periodicity, as shown in red arrow in Fig. 1). The Al-SWG modulates the lateral (x-direction) wavenumber of the diffracted light by the factor of $2\pi m/\Lambda$ (m is diffraction order)¹¹. The lateral wavenumbers of 0th order diffractions ($m = 0$) are not changed by the grating. On the other hand, all higher order diffractions ($m \neq 0$) become evanescent wave propagating along the interface between the SWG and ITO layer because of the large wavenumber modulation of the SWG. The matching of the wavenumbers between the higher orders and the waveguide modes in the ITO layer causes the excitation of the guided-modes propagating along x-direction in ITO. The excited guided-mode propagates along ITO layer with internal reflections at ITO-glass and the SWG-ITO interfaces, and the mode partially leaks to the incident region by the Al-SWG. If the leaked mode and the 0th reflected diffraction are in-phase and constructively interfere each other, the peak can be obtained resonantly in its reflection spectrum. We find the more detail of the phase relation between leaked guided-mode and the 0th diffraction in the literature¹².

When we apply the external magnetic field for the sample during the current flowing into the ITO layer, the induced Lorentz-force accumulates the electrons to the upper side of the ITO layer. The electron concentration of the accumulation layer depends on the magnetic field because the Lorentz-force is proportional to the field strength, and the concentration also influences strongly on the refractive index (RI) of the accumulation layer¹³. The intensity of the reflection peak resulting from the guided-mode is varied by the concentration of accumulation layer because the phase change of the mode at the SWG-ITO interface reflection depends on the RI of accumulation layer. As a result, the peak intensity varies with the applied magnetic field. The accumulation is vanished when the magnetic field and current disappear, and the accumulation vanishing has no hysteresis characteristic. Hence, we can measure the applied magnetic field without degaussing. In order to coincide the wavenumber of ± 1 st diffractions with the guided-mode at the wavelength of 630 nm, we set structural parameters to $\Lambda = 400$ nm, $w = 200$ nm, $t_{ITO} = 180$ nm, $t_{SWG} = 30$ nm, respectively.

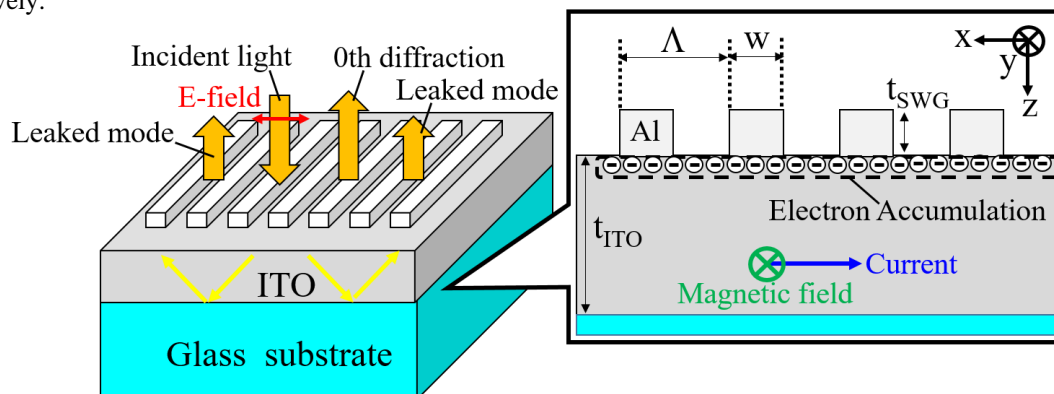


Figure 1. Schematic of our proposed Al-SWG on ITO layer structure. The enlarged figure is sketch of the accumulation layer induced by Lorentz-force.

We also fabricated the designed Al-SWG on the ITO film. We used a 180 nm thickness ITO film deposited on the glass substrate by sputtering technique (ITO Coated Glass, 10 mm x 10 mm x 0.7 mm: MTI Co.). The EB resist film (ZEP-520A: Zeon Co.) was spin-coated onto the sample surface. The spin coating time and rotation speed were optimized so that the resist film thickness was about 100 nm. The SWG pattern was exposed by EB lithography with 50 kV. After development of the SWG pattern on the sample (ZED50N: Zeon Co.), 30 nm Al film was EB evaporated onto the patterned resist. Finally, the resist was removed by dimethyl sulfoxide solution. The region size of the fabricated SWG is 300 μm x 300 μm . Figure 2 shows the scanning electron microscope (SEM) image of the fabricated sample surface. The Al-SWG has 400 nm period and 200 nm bar width, respectively.

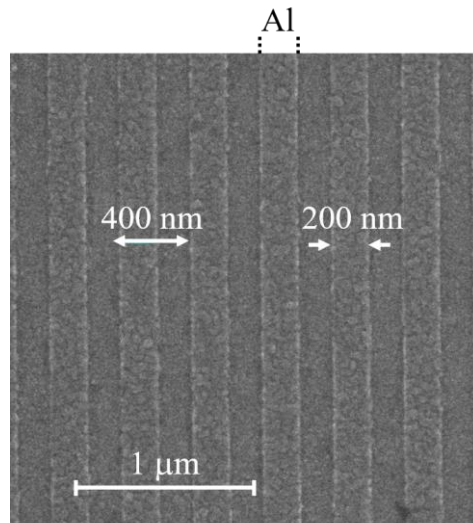


Figure 2. SEM image of the 30 nm Al-SWG on ITO layer. The scale bar corresponds to 1 μm . The Al-SWG has 400 nm period and 200 nm grating bar width.

3. RESULTS AND DISCUSSION

We experimentally characterized the spectral property and magnetic field dependence of the fabrication sample. We employed halogen lamp as broadband visible light source. The light emitted from halogen lamp was p-polarized light (the electric field is perpendicular to grating fingers), and the light was focused on the Al-SWG region by using objective lens ($\times 20$, $\text{NA} = 0.4$). The reflected intensities were detected by commercialized spectrometer (OP-Flame-S Package: Ocean Photonics Co.). The measured spectra of the ITO film without and with the Al-SWG were shown in Fig 3 (a) and (b), respectively. The values of the reflectivity were evaluated based on that of the reference Al mirror (TFA-50C08-4: Sigma Co.). We cannot find the reflection peak in its wavelength spectrum of the ITO without the Al-SWG, whereas the peak around the wavelength of 615 nm appears in that with the SWG. The experimental peak wavelength is slightly different from that predicted (630 nm). This deviation can attribute to the rough surface of the fabricated Al-SWG (See Fig. 2) because the imperfectness provides the fluctuation of the guided-mode phase.

We also investigated the magnetic field response of the peak intensity. A neodymium magnets were placed on the side of the sample to apply the magnetic field (the direction of magnetic field is same as that in Fig. 1). We flowed the current of 100 mA in ITO layer, whose sample size 1 cm x 1 cm in order to form the accumulation layer at the SWG-ITO interface. Figure 4 (a) and (b) show the dependences of the intensities at peak wavelength (615 nm) on the applied magnetic field values. The magnetic field values were measured by commercialized gauss meter (Gaussmeter 410: Lake Shore Co.). For the ITO without the Al-SWG (Fig. 4(a)), the intensity at the wavelength of 615 nm shows almost no change by applied magnetic field value up to 172 mT. On the other hand, the peak intensity of the sample with Al-SWG significantly decreases with the increasing value of the applied magnetic field (Fig. 4 (b)). The relative reflectivity change with applying magnetic field of 172 mT reaches to about 3 % of that without magnetic field. In particular, we obtain the high sensitivity of about 0.0466%/mT around the 138 mT to 172 mT region. Moreover, the peak intensity almost return to the original value before current flowing and magnetic field applying when the current and magnetic field disappeared (the open circle

in Fig. 4 (b)). These results indicate that our sample can measure tens of mT magnetic field without degaussing process (assuming 1% detection limit of spectrometer).

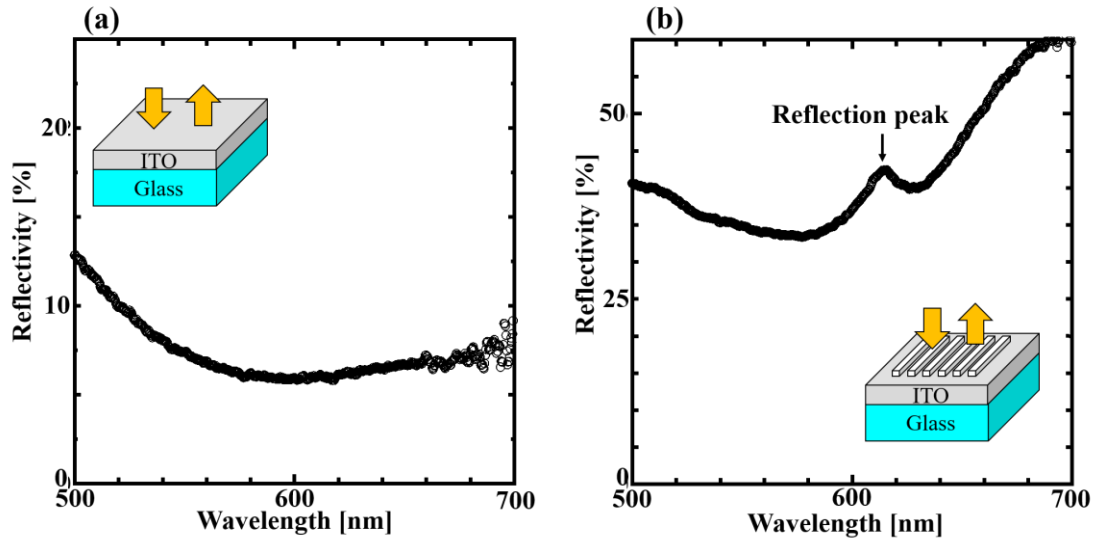


Figure 3. Normal reflection spectra of the ITO layer (a) without (b) with the Al-SWG.

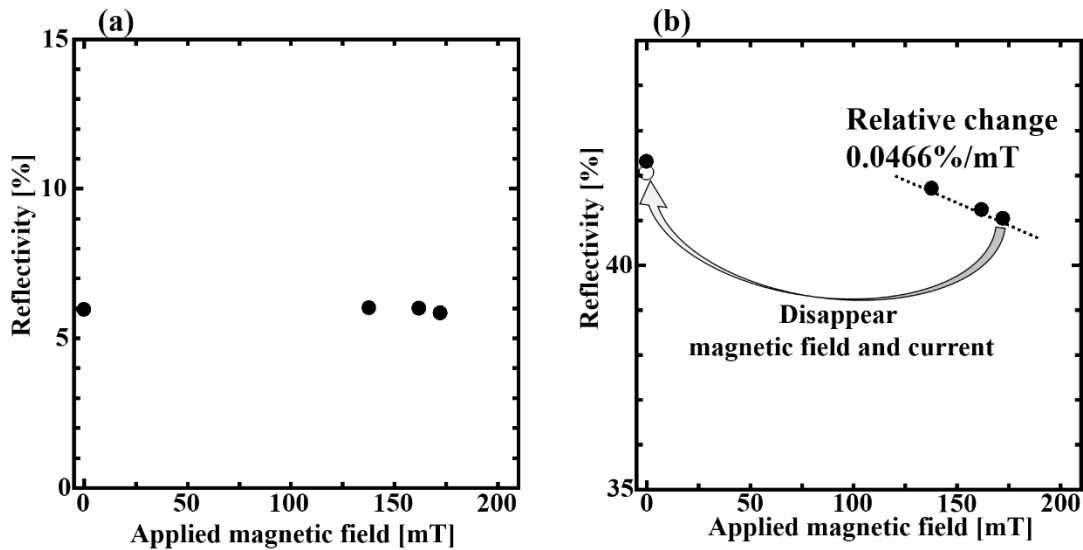


Figure 4. Magnetic field dependence of the reflectivity (the wavelength of 615 nm) of the ITO layer (a) without (b) with the Al-SWG. The open circle indicates the reflectivity when the magnetic field and the current disappear after measurements.

We also calculated the electromagnetic field distribution using FDTD method for discussing the light behavior in the Al-SWG on ITO layer with the accumulation layer. The FDTD calculation model is the same as the optical configuration shown in Fig. 1, and the p-polarized plane wave of the 615 nm wavelength enters normally to the sample. We assumed that the structure infinitely repeats for x-direction. The calculation spatial grid size and time interval were 1 nm and 2.31×10^{-17} s, respectively. RI values of Al were taken from previous literatures¹⁴, and the value of commercial glass (D 263 T eco Thin Glass: SCHOTT Co.) is used as glass substrate. We employed 1.9 as RI value of the ITO film at the wavelength of 615 nm from its experimental thin-film interference reflection spectrum. The RI of accumulation layer in ITO n_{ITO} (accumulation layer) is also given by as follow equation¹³.

$$n_{ITO(\text{accumulation layer})} = \sqrt{\epsilon_{\infty} - \frac{\omega_p^2}{\omega^2 + i\omega\Gamma}} \quad (1)$$

Where, the symbols ω , ϵ_{∞} , Γ , are angular frequency of the incident light, background dielectric constant, frequency of collision (namely, damping), respectively. The symbol ω_p is plasma angular frequency, which defined by $nq^2/\epsilon_0 m^*$, and q , n , ϵ_0 , m^* are charge of electron, permittivity in vacuum, effective mass of electron respectively. To estimate roughly the behavior of light in our structure, we employed typical values, such as $\epsilon_{\infty} = 4$, $\Gamma = 1.53 \times 10^{14}$ rad/s., $m^* = 0.35 m_0$ (m_0 is rest mass of the electron)¹⁵. The electron concentration of the ITO layer of our sample is $6.2 \times 10^{20} \text{ cm}^{-3}$ that estimated by its sheet resistance. The thickness of the accumulation layer at the SWG and ITO interface is assumed to be 2 nm¹⁶, and the accumulation electron density of $5.58 \times 10^{22} \text{ cm}^{-3}$ is used because we assumed the electrons in ITO layer concentrates into the 2 nm accumulation layer. According to eq. (1), the RI value of the accumulation layer $5.58 \times 10^{22} \text{ cm}^{-3}$ concentration is $0.189 + 7.07i$ at the wavelength of 615 nm.

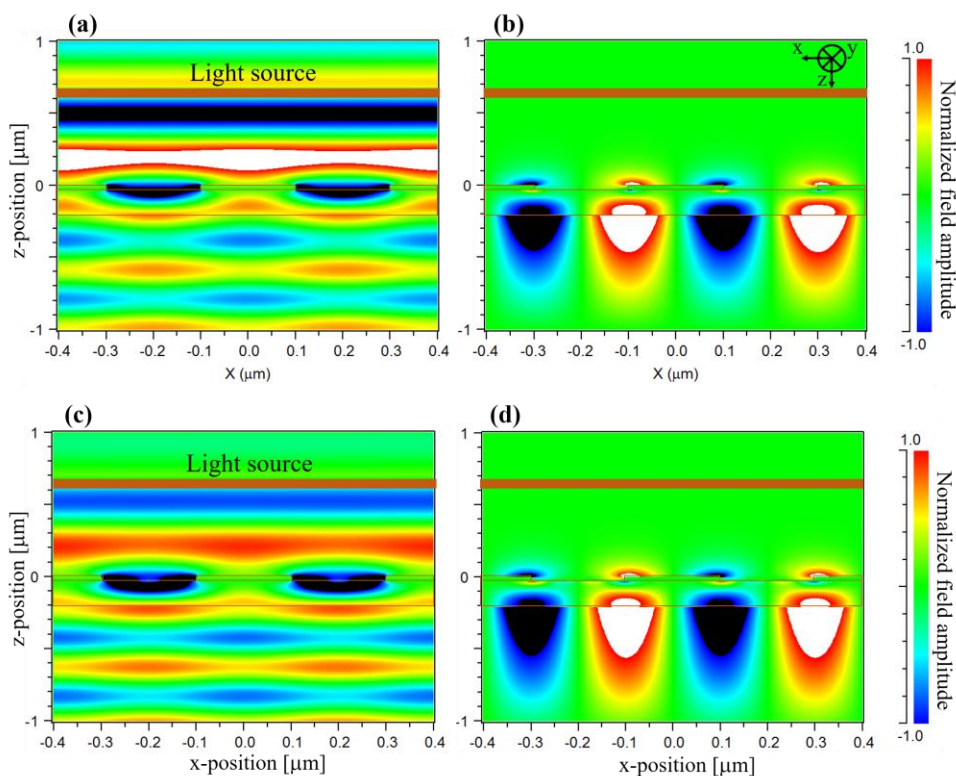


Figure 5. (a) and (b) show E_x and E_z components of electric field distribution of Al-SWG on ITO layer without the accumulation; (c) and (d) show these components with the accumulation layer at the SWG and ITO interface.

Figure 5(a), (b) and (c), (d) show the x - and z -components of the electric field distributions (E_x and E_z) of our structure without and with accumulation layer, respectively. The amplitudes were normalized by that of the incident light. The brown square is light source, and the light propagates along $+z$ -direction. The E_x component distribution without accumulation (Fig. 5 (a)) is distorted and the high field appears incident region around the top of the Al-SWG. We can also find E_z component only in the ITO layer despite of z -direction incidence, and the field is confined in ITO layer (Fig. 5 (b)). The distributions indicate that the Al-SWG excites the photonic mode propagating along ITO layer, namely guided-mode, and the 0th reflected diffraction and the leaked guided-mode constructively interferes and enhances each other. Thus, high reflected field appears in the incident region, and the field distribution agree with the experimental fact that we obtained the reflection peak.

The field profiles around the SWG and ITO interface is significantly varied by the only 2nm thickness of the accumulation layer, as shown in Fig. 5 (c) and (d). This means the phase of the guided-mode at the SWG and ITO interface is varied by the accumulation layer. As a result, the constructive interference condition is also changed, and the reflected field become weaker than that without the accumulation (Fig. 5 (c)). The calculated tendency of the light behavior shows good agreement with the experimental one. The reason why the accumulation layer with only 2nm thickness has large effect on the reflection peak intensity can be explained as follows. The guided-mode propagates along ITO, and the phase also changes at internal reflection of the SWG-ITO and ITO-glass substrate¹². These phase change determines the phase difference between the 0th diffraction and the leaked guided-mode. If the accumulation layer exists at the SWG and ITO layer interface, the phase change at the interface slightly deviates from that without the accumulation. The deviation gradually increases at each reflection of the mode at the interface as it propagates along ITO. Thus, very thin accumulation layer has large influence on the interference, and the spectrum also strongly depend on the accumulation layer.

4. CONCLUSION

In conclusion, we experimentally demonstrated the degaussing-free magnetic field sensing using Al-SWG on ITO layer. The structural geometry of the SWG was designed to excite the guide-mode in ITO layer. The designed structure was fabricated by EB lithography technique, and the sample showed the resonant reflection peak resulting from the guide-mode excitation. The peak reflectivity significantly decreased owing to appearance of the accumulation layer in ITO layer induced by applying magnetic field and flowing current. The relative decreasing of the reflectivity at 172 mT reached to 3% of that without the current and the magnetic field. When the current and magnetic field disappeared, the reflection peak intensity almost returned to the original value before current flowing and magnetic field applying. The results indicates our structure can measure tens of mT magnetic field without degaussing, and ease of measurement of our sensor is very useful for IoT applications. Also, the FDTD field calculation clarified the influence of the accumulation layer on the guided-mode propagation. The results provide new devices concept of optical spectral control with magnetic field, and is very interesting for other fields, for example communication.

ACKNOWLEDGMENTS

This work is partially supported by JSPS KAKENHI Grant Number JP18K04238.

REFERENCES

- [1] Girgin, A. and Karalar, T. C., "Output offset in silicon Hall effect based magnetic field sensors," *Sens. Actuators A* 288, 177-181 (2019).
- [2] Guedes, A., Macedo, R., Jaramillo, G., Cardoso, S., Freitas, P. P. and Horsley, D. A., "Hybrid GMR sensor detecting 950 pT/sqrt(Hz) at 1 Hz and room temperature," *Sensors* 18(3), 790 (2018).
- [3] Gallop, J., "SQUIDS: some limits to measurement," *Supercond. Sci. Technol.* 16(12), 1575-1582 (2003).
- [4] Gangwar, R. K., Bhardwaj, V. and Singh, V. K., "Magnetic field sensor based on selectively magnetic fluid infiltrated dual-core photonic crystal fiber," *Opt. Eng.* 55(2), 026111 (2016).
- [5] Bao, L., Dong, X., Zhang, S., Shen, C. and Shum, P. P., "Magnetic field sensor based on magnetic fluid-infiltrated phase-shifted fiber Bragg grating," *IEEE Sens. J.* 18(10), 4008-4012 (2018).
- [6] Lei, X., Chen, J., Shi, F., Chen, D., Ren, Z. and Peng B., "Magnetic field fiber sensor based on the magneto-birefringence effect of magnetic fluid," *Opt. Commun.* 374, 76-79 (2016).
- [7] Li, Z., Liao, C., Song, J., Wang, Y., Zhu, F., Wang, Y. and Dong, X., "Ultrasensitive magnetic field sensor based on an in-fiber Mach-Zehnder interferometer with a magnetic fluid component," *Photon. Res.* 4(5), 197-201 (2016).
- [8] Takashima, Y., Haraguchi, M. and Naoi, Y., "Highly sensitive magnetic field sensor with normal-incidence geometry using Ni-based bilayer subwavelength periodic structure operating in visible-wavelength region," *Jpn. J. Appl. Phys.* 57(8S2), 08PE01 (2018).
- [9] Takashima, Y., Haraguchi, M. and Naoi, Y., "Optical magnetic field sensor based on guided-mode resonance with Ni subwavelength grating/waveguide structure," *Proc. SPIE* 10928, 109281S (2019).

- [10] Takashima, Y., Moriwa, K., Haraguchi, M. and Naoi, Y., "Ni subwavelength grating/SiO₂/Ag based optical magnetic field sensor with normal incident geometry," Proc. SPIE, 11089, 110891V (2019).
- [11] Kikuta, H., Toyota, H. and Yu, W., "Optical elements with subwavelength structured surface," Opt. Rev. 10(2), 63-73 (2003).
- [12] Sahoo, P. K., Sarkar, S. and Joseph, J., "High sensitivity guided-mode-resonance optical sensor employing phase detection," Sci. Rep. 7, 7607 (2017).
- [13] Liu, X., Zang, K., Kang, J. H., Park, J., Harris, J. S. Kik, P. G. and Brongersma, M. L., "Epsilon-near-zero Si slot-waveguide modulator," ACS Photonics 5(11), 4484-4490 (2018).
- [14] McPeak, K. M., Jayanti, S. V., Kress, S. J. P., Meyer S., Iotti, S., Rossinelli, A. and Norris, D. J., "Plasmonic films can easily be better: rules and recipes," ACS Photonics 2(3), 326-333 (2015).
- [15] Hamberg, I. and Granqvist, C. G., "Evaporated Sn-doped In₂O₃ films: basic optical properties and applications to energy-efficient windows," J. Appl. Phys. 60(11), R123-R160 (1986).
- [16] Huang, Y. W., Lee, H. W. H., Sokhoyan, R., Pala, R. A., Thyagarajan, K., Han, S., Tsai, D. P. and Atwater, H. A., "Gate-tunable conducting oxide metasurface," Nano Lett. 16(9), 5319-5325 (2016).